



Geophysical Research Letters*



RESEARCH LETTER

10.1029/2021GL093405

Special Section:

Fire in the Earth System

Key Points:

- CrIS is able to detect PANs and CO enhancements in smoke plumes from many wildfires during the 2018 wildfire season
- We estimate that the average contribution from wildfire to tropospheric PANs over the western U.S. is 19–56% during the 2018 wildfire season
- Near source PANs photochemical production rates can be observed using CrIS measurements of PANs and CO

Supporting Information:

Supporting Information may be found in the online version of this article.

Correspondence to:

J. F. Juncosa Calahorrano, jjuncosa@colostate.edu

Citation:

Juncosa Calahorrano, J. F., Payne, V. H., Kulawik, S., Ford, B., Flocke, F., Campos, T., & Fischer, E. V. (2021). Evolution of acyl peroxynitrates (PANs) in wildfire smoke plumes detected by the Cross-Track Infrared Sounder (CrIS) over the western U.S. during summer 2018. *Geophysical Research Letters*, 48, e2021GL093405. https://doi.org/10.1029/2021GL093405

Received 19 MAR 2021 Accepted 7 JUL 2021

© 2021. The Authors.

This is an open access article under the terms of the Creative Commons Attribution License, which permits use, distribution and reproduction in any medium, provided the original work is properly cited.

Evolution of Acyl Peroxynitrates (PANs) in Wildfire Smoke Plumes Detected by the Cross-Track Infrared Sounder (CrIS) Over the Western U.S. During Summer 2018

Julieta F. Juncosa Calahorrano¹, Vivienne H. Payne², Susan Kulawik³, Bonne Ford¹, Frank Flocke⁴, Teresa Campos⁴, and Emily V. Fischer¹

¹Department of Atmospheric Science, Colorado State University, Fort Collins, CO, USA, ²Jet Propulsion Laboratory, California Institute of Technology, Pasadena, CA, USA, ³Bay Area Environmental Research Institute/NASA Ames, Moffett Field, CA, USA, ⁴National Center for Atmospheric Research, Fort Collins, CO, USA

Abstract We use observations of acyl peroxynitrates (PANs) from the Cross-Track Infrared Sounder (CrIS) to investigate PANs over the western U.S. during the summer 2018 wildfire season. This period coincides with the Western Wildfire Experiment for Cloud Chemistry, Aerosol Absorption, and Nitrogen (WE-CAN). When combined with favorable background conditions, the resolution and sensitivity of CrIS is sufficient to observe the production of PANs in smoke plumes. CrIS PANs normalized excess mixing ratios with respect to CO (NEMRs) in the Pole Creek Fire increase from 0.2% to 0.4% within 3–4 hr of physical aging, consistent with in situ NEMRs. CrIS is also able to detect PANs enhancements in plumes that have been transported hours to days downwind. On average for summer 2018, 19–56% of PANs in the free troposphere during the afternoon over the western U.S. can be attributed to smoke.

Plain Language Summary Wildfire smoke contains nitrogen compounds, such as nitrogen oxide radicals, that participate in ozone chemistry and degrade air quality. Acyl peroxynitrates, also known as PANs, are formed rapidly in wildfire plumes and serve as temporary reservoirs for nitrogen oxide radicals. At colder temperatures, PANs can transport nitrogen oxides very long distances before releasing them again to the atmosphere. Here we discuss the detection of PANs in wildfire smoke using new measurements from the Cross-Track Infrared Sounder (CrIS). We find that CrIS is able to detect high concentrations of PANs in smoke plumes from fast-growing fires. The instrument is also able to detect the chemical production of PANs within a given smoke plume and the production rates are comparable with aircraft observations during the Western Wildfire Experiment for Cloud Chemistry, Aerosol Absorption, and Nitrogen (WE-CAN). Our results highlight the importance of wildfires as a source of PANs in the midlatitudes and show the potential of satellite retrievals to compliment campaign-based observations of PANs.

1. Introduction

Acyl peroxynitrates (PANs) are thermally unstable reservoir species for nitrogen oxide radicals ($NO_x = NO + NO_2$) that can be transported over long distances to affect photochemical processes far from NO_x emission sources (Singh, 1987; Singh & Hanst, 1981). Smoke contains high concentrations of PANs precursors (Akagi et al., 2011; Bond et al., 2004; Crutzen & Andreae, 1990; Fearnside et al., 1993), and rapid formation of PANs occurs in smoke plumes (Akagi et al., 2011; Alvarado et al., 2010; Juncosa Calahorrano et al., 2020; Lindaas et al., 2020; Liu et al., 2016; Yokelson et al., 2009) temporarily sequestering a large fraction of the NO_x emitted from fires. Wildfire smoke is often injected into the free troposphere, allowing the PANs produced within smoke plumes to travel long distances, redistributing NO_x and impacting ozone (O_3) chemistry far from the fire source (e.g., Brey & Fischer, 2016; Lindaas et al., 2017; Singh et al., 2012). Thus, understanding the abundances and chemistry of PANs in wildfire smoke is essential to quantifying the contribution of wildfires to regional and global NO_x and O_3 abundances.

Existing in situ measurements of PANs within wildfire plumes (e.g., Akagi et al., 2011; Alvarado et al., 2015; Baylon et al., 2015; Briggs et al., 2017; Fischer et al., 2014; Juncosa Calahorrano et al., 2020; Liu et al., 2016; Yokelson et al., 2009) cover a relatively limited number of plumes, often do not provide information over the full spatial extent of individual plumes (i.e., extending from the source fire downwind), and provide limited temporal coverage (i.e., observations are campaign-based, covering weeks to months). New satellite observations of



PANs offer a complementary perspective (Payne et al., 2014). PAN observations from the Tropospheric Emission Spectrometer (TES) on the Aura satellite demonstrated that summertime satellite-measured PAN enhancements over North America are often (15–32% of the time) associated with smoke plumes, specific instances of elevated PAN can be connected to specific fire complexes, and that within-plume enhancements ratios of PAN relative to carbon monoxide (CO) fall within the range calculated from in situ observations (Fischer et al., 2018).

The Cross-Track Infrared Sounder (CrIS) has flown on the Suomi National Polar-orbiting Partnership (Suomi NPP) satellite since 2011. CrIS offers an opportunity to continue and expand the PANs observational record established by TES. Here, we summarize CrIS retrievals collected over a portion of the summer 2018 North American wildfire season coinciding with the Western Wildfire Experiment for Cloud Chemistry, Aerosol Absorption, and Nitrogen (WE-CAN). We isolate smoke-impacted retrievals using multiple methods, estimate the fraction of PANs in the free troposphere over the western U.S. that can be attributed to smoke, calculate enhancements in PANs relative to CO, and compare our calculations with those based on in situ data from WE-CAN.

2. Methods

2.1. CrIS Observations

The Suomi NPP satellite is on a sun-synchronous Earth orbit with overpass times around 01:30 and 13:30 local time (LT). CrIS is a nadir viewing Fourier transform spectrometer (FTS) that measures thermal infrared radiances with high spectral resolution (0.625 cm⁻¹). The CrIS PANs retrievals rely on the PANs absorption feature at 790 cm⁻¹. The spectral feature at 790 cm⁻¹ appears in the IR spectra of all acyl peroxynitrates (PANs) at essentially the same frequency given the relatively broad nature of this absorption band. Thus, the measurements presented here are for all the PANs compounds (i.e., they include propionyl peroxynitrate (PPN; CH3CH2C(O) OONO2), methacryloyl peroxynitrate (MPAN; CH2C(CH3)C(O)OONO2), etc.) in addition to PAN (CH3C(O) O2NO2). The retrieval algorithm uses the Multi-Species, Multi-Spectral, Multi-Satellite (MUSES) retrieval software (Fu et al., 2016), which builds on the optimal estimation algorithm developed for Aura-TES (Beer et al., 1999; Bowman et al., 2006). CrIS PANs retrievals are performed from NASA v2 Level 1B radiances (Revercomb & Strow, 2019) on the 15 km individual fields of view (FOVs). These CrIS PANs and CO retrievals are described in Payne et al. (2021) and Fu et al. (2016), respectively. Simulations suggest that the single FOV detection limit for CrIS PANs is <0.15 ppbv.

For this analysis, we present a tropospheric average for each PANs and CO retrieval. For this study, this is defined as the average retrieved PANs and CO between the 825 and 215 hPa. CrIS sensitivity to PANs is higher in the free troposphere (<680 hPa), and it decreases rapidly near the surface. The CO and PANs averaging kernels in Figure S1 in Supporting Information S1 show that CrIS is more sensitive to CO than to PANs (see Text S1 in Supporting Information S1). In our comparisons to in situ data collected during WE-CAN, we compare the CrIS retrievals to the sum of PAN and PPN.

To avoid biases associated with silica spectral features in surface emissivity (i.e., bare sandy or rocky surfaces), we exclude geographic areas identified with such surfaces. There is a silica feature in surface emissivity around $1,150~\rm cm^{-1}$, with a weaker feature $790~\rm cm^{-1}$ that coincides with the PANs feature utilized here. Deserts are denoted in the CrIS data products used here when the average emissivity at $1,025~\rm cm^{-1}$ is less than 0.95. We eliminate any retrievals within $0.5^{\circ} \times 0.5^{\circ}$ cells where the average Desert QA flag <0.95 and the percent of negative PANs value >40%. All the geographic regions excluded based on these criteria are listed in Table S1 and shown in Figure S2 in Supporting Information S1 (e.g., Moab, Death Valley, etc.). We found that these criteria are insufficient to remove areas on the edges of Desert regions (see Figure S3 in Supporting Information S1). Thus, we chose to also remove any remaining negative PANs values from this analysis. This final step removes ~15% of the data, primarily from regions that border deserts (See Figure S3 in Supporting Information S1).

2.2. NOAA Hazard Mapping System (HMS) Fire and Smoke Product

We use the National Oceanic and Atmospheric Administration (NOAA) HMS to identify smoke-impacted CrIS retrievals (Rolph et al., 2009). Using visible imagery from seven satellites, trained satellite analysts generate a daily (daytime) operational outline of smoke plumes (Ruminski et al., 2006). Smoke detections are manually inspected, and contours are drawn depicting approximate surface smoke concentrations without information on the



vertical location of the smoke. We use archived HMS shapefiles (https://satepsanone.nesdis.noaa.gov/pub/FIRE/HMS/) that are gridded to a $0.5^{\circ} \times 0.2^{\circ}$ horizontal resolution with the maximum smoke concentration value for a given location on a given day.

2.3. HYSPLIT Trajectories

We use the Hybrid Single Particle Lagrangian Integrated Trajectory (HYSPLIT) model (Draxler & Hess, 1998) to estimate the origin and age of a small subset of smoke plumes. For this application, the HYSPLIT model uses the North American Regional Reanalysis (NARR) meteorological product. NARR has a time step of 3 hr, a grid spacing of 32 × 32 km, and 23 vertical layers between the surface and 100 hPa. We initialized a set of forward and backward trajectories for a period of 24 hr at the locations of smoke-impacted CrIS retrievals. All trajectories were initialized at 720, 600, and 495 hPa levels. Details are provided in Section 3.3.

2.4. Classification of Smoke-Impacted Retrievals

We classify smoke-impacted retrievals using satellite observations in two ways and analyze them separately. (1) The HMS criteria uses the *cdist* tool in the Python 3.7.6 *scipy.spatial.distance* (*scipy version 1.4.1*) package to colocate the CrIS retrievals with the NOAA HMS smoke plumes (Figure S4 in Supporting Information S1). (2) The CrIS criteria includes retrievals where CrIS CO > 150 ppbv at the 510 or 680 hPa level, following Fischer et al. (2018) (see Figure S5 in Supporting Information S1). Results from sensitivity analysis on the CrIS smoke criteria are discussed in the text associated with Table S2 in Supporting Information S1.

2.5. Physical Age Calculations

In Section 3.3, we assign a physical age to each CrIS retrieval in the Pole Creek Fire plume based on the visible images from GOES-16 and HYSPLIT trajectories initiated at the time of the satellite overpass (21:00 UTC). A visual inspection of satellite images and the trajectory analysis concur that the front edge of the plume is 3–4 hr old at 21:00 UTC. We calculate the distance from each retrieval to the fire centroid for that day as reported by Inciweb (https://inciweb.nwcg.gov/). Finally, we calculate an average plume wind speed dividing the distance of the furthest smoke-impacted CrIS retrieval by the range of ages of the front edge of the plume. This yields average wind speeds between 19 and 26 m s⁻¹. Using the lower estimate for wind speed (closest estimate to visual imagery from GOES-16), we estimate the age of each in-smoke CrIS retrieval.

3. Results

3.1. Western U.S. CrIS PANs Retrievals and Wildfire Smoke

During 2018, there were 23,104 wildfires in the western U.S. corresponding to a burned area of >6.5 million acres (https://www.nifc.gov/nicc/index.html). Figure 1 shows CrIS retrievals of CO (Figure 1a) and PANs (Figure 1c) on August 20, 2018 when the Mendocino Complex Fire was active. Figure 1 shows that many fires (red dots) can be active on a given day and that CrIS has the ability to detect CO and PANs from individual smoke plumes. This is in contrast to the TES PAN retrievals which can only be interpreted in aggregate (Fischer et al., 2018).

Figure 1 shows that PANs and CO enhancements from the wildfires cross many western states, and that the smoke plumes from some wildfires are detectable multiple days downwind. Many of the smoke plumes sampled during WE-CAN were also detected by CrIS (e.g., Carr Fire, South Sugarloaf Fire smoke plumes). Within the lifecycle of a wildfire, the CrIS overpass time at ~1:30 p.m. LT (~19:30–20:30 UTC) often occurs before many wildfires are most active and produce the largest emissions (Mu et al., 2011). The WE-CAN sampling efforts most often intercepted fresh plumes between 3 and 6 p.m. LT (21:00–01:00 UTC). Therefore, there is often a ~2–5 hr difference between the satellite overpass and the in situ measurements. Full details on the WE-CAN are found in Juncosa Calahorrano et al. (2020).

Figures 1b and 1d show the aircraft sampling of the plume associated with the Mendocino Complex Fire. The Mendocino Complex Fire was first active on July 27, 2018 and was not contained until mid-September 2018. On August 20, 2018, the NSF/NCAR C-130 sampled the smoke plume in a pseudo-Lagrangian fashion, completing multiple transects across the plume. In situ PANs (CO) abundances at the core of the Mendocino Complex smoke



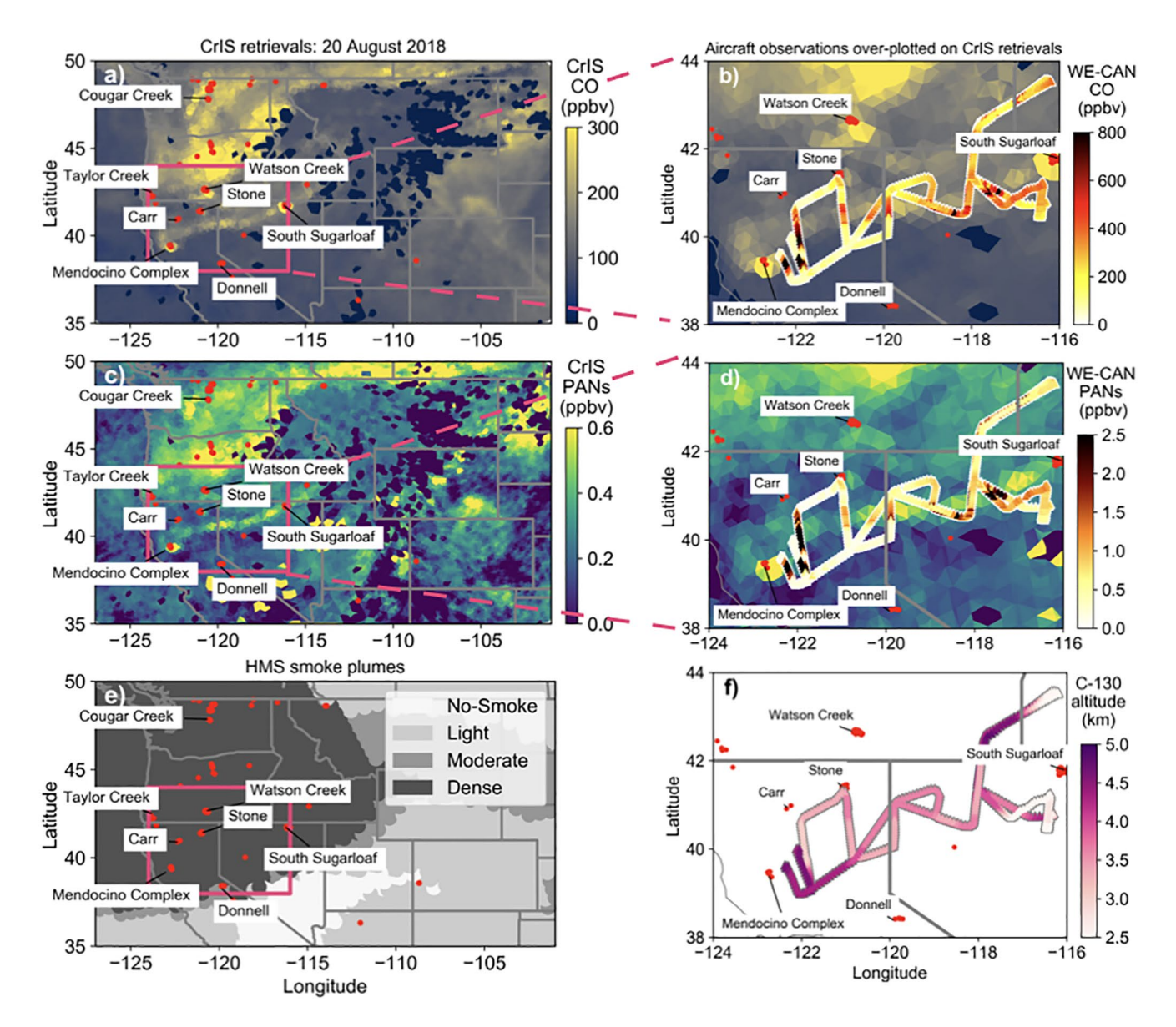


Figure 1. Maps of Cross-Track Infrared Sounder (CrIS) (a) CO and (c) peroxynitrates (PANs) measurements of the Mendocino Complex Fire smoke plume (left) with in situ observations of (b) CO and (d) PANs (PAN + PPN) from the same fire over-plotted (right) for a smaller inset region (pink box on left-hand plots). (e) Hazard Mapping System (HMS) smoke plumes (i.e., light, moderate, dense) and (f) altitude of the in situ measurements in km above sea level. Fires detected by the Visible Infrared Imaging Radiometer Suite (VIIRS) on the Suomi Suomi National Polar-orbiting Partnership (Suomi NPP) on this day are shown as red dots (https://earthdata.nasa.gov/firms).

plume ranged from 3.3 to 7.5 ppbv (700–2,000 ppbv), and the plume was sampled between 610 and 570 hPa (4.1–4.6 km ASL). CrIS free tropospheric average PANs (CO) mixing ratios within the plume ranged from 0 to 1.4 ppbv (100–2,900 ppbv).

3.2. CrIS PANs Abundances Within and Outside Wildfire Smoke Plumes

Figure 2 presents a summary of smoke-impacted and smoke-free tropospheric average PANs and CO CrIS retrievals designated using the CrIS and HMS smoke criteria. Based on the CrIS criteria alone, only ~35% of the retrievals are classified as smoke-impacted, while the HMS criteria classifies ~70% of the retrievals as smoke-impacted. Figure 2 shows the distributions of PANs and CO in these two data subsets (see Figure S6 in Supporting Information S1 for distributions of light, moderate, and dense smoke for the HMS criteria and different CO thresholds for the CrIS criteria). The mean PANs and CO in the smoke-impacted CrIS retrievals is significantly different



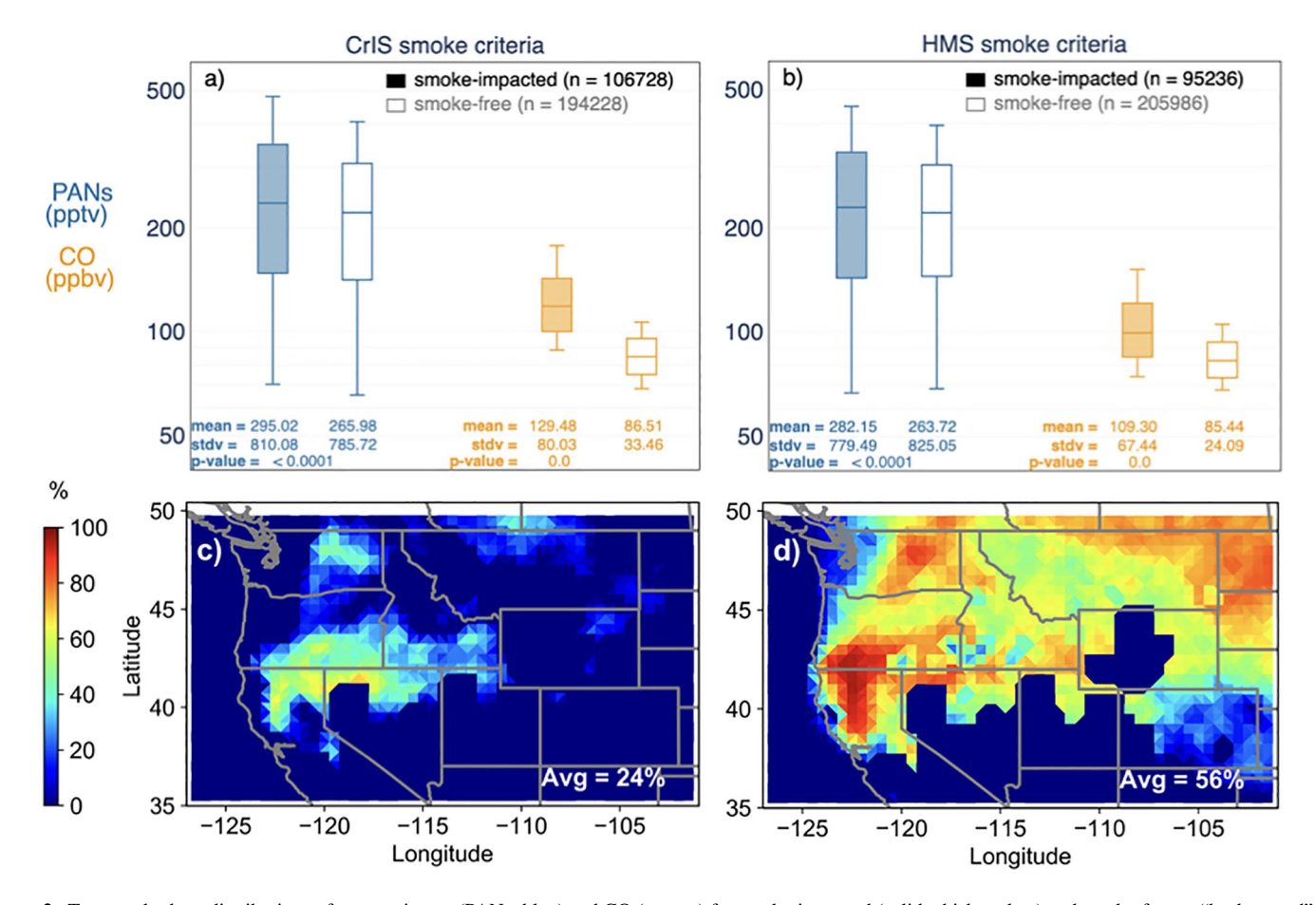


Figure 2. Top panels show distributions of peroxynitrates (PANs; blue) and CO (orange) for smoke-impacted (solid whisker plots) and smoke-free or "background" (open whisker plots) retrievals identified using (a) the Cross-Track Infrared Sounder (CrIS) and (b) the Hazard Mapping System (HMS) smoke criteria (see Section 2.4) for the study period (July 24 to September 13, 2018). *Note* the logarithmic *y* axes. The boxes enclose the 25th to 75th percentiles, the whiskers represent the 10th and 90th percentiles, and the horizontal bar represents the median. The number next to the solid and open squares corresponds to the number of individual retrievals in each category. Bottom panels show percent of PAN attributed to regional wildfires based on the (c) CrIS and (d) HMS smoke criteria.

(larger) than the mean PANs and CO in the smoke-free retrievals based on *t* tests. Differences were not significant in smoke-free versus smoke-impacted TES retrievals (Fischer et al., 2018).

The designation of background is important for quantifying the contribution of wildfire smoke to the abundance of a species within a given air mass and separating chemical processes from dilution (Yokelson et al., 2009). In the following section, we assume background tropospheric average mixing ratios for PANs and CO of 0.13 and 90 ppbv, respectively. These choices approximately represent the lowest 25th percentile for PANs and the median value for CO for the smoke-free distributions in Figure 2 and are within the range used by Fischer et al. (2018).

To assess the percentage of the PANs retrieved by CrIS attributed to fires, we subtract a weighted average of the smoke-free retrievals from a weighted average of the smoke-impacted retrievals (see Figure S7 and Equations 1 and 2 in Supporting Information S1 for details). The percent smoke contribution using the CrIS and the HMS criterion are shown in Figures 2c and 2d, respectively. Both criteria indicate that most of the free tropospheric PANs (40–100%) over northern California are associated with smoke, largely attributed to the Mendocino Complex and Carr Fires (see Table S2 in Supporting Information S1 for details). The smoke contribution to tropospheric PANs based on the HMS criteria extends from Northern California and Southern Oregon to the northeast of the region of study. Averaged across the whole region in Figures 2c and 2d, the CrIS (HMS) criteria attributes 24% (56%) of the tropospheric PANs to smoke. Table S2 in Supporting Information S1 shows that the CrIS criteria can attribute between 19% and 39% of the tropospheric PANs to smoke depending on the threshold chosen for CO.



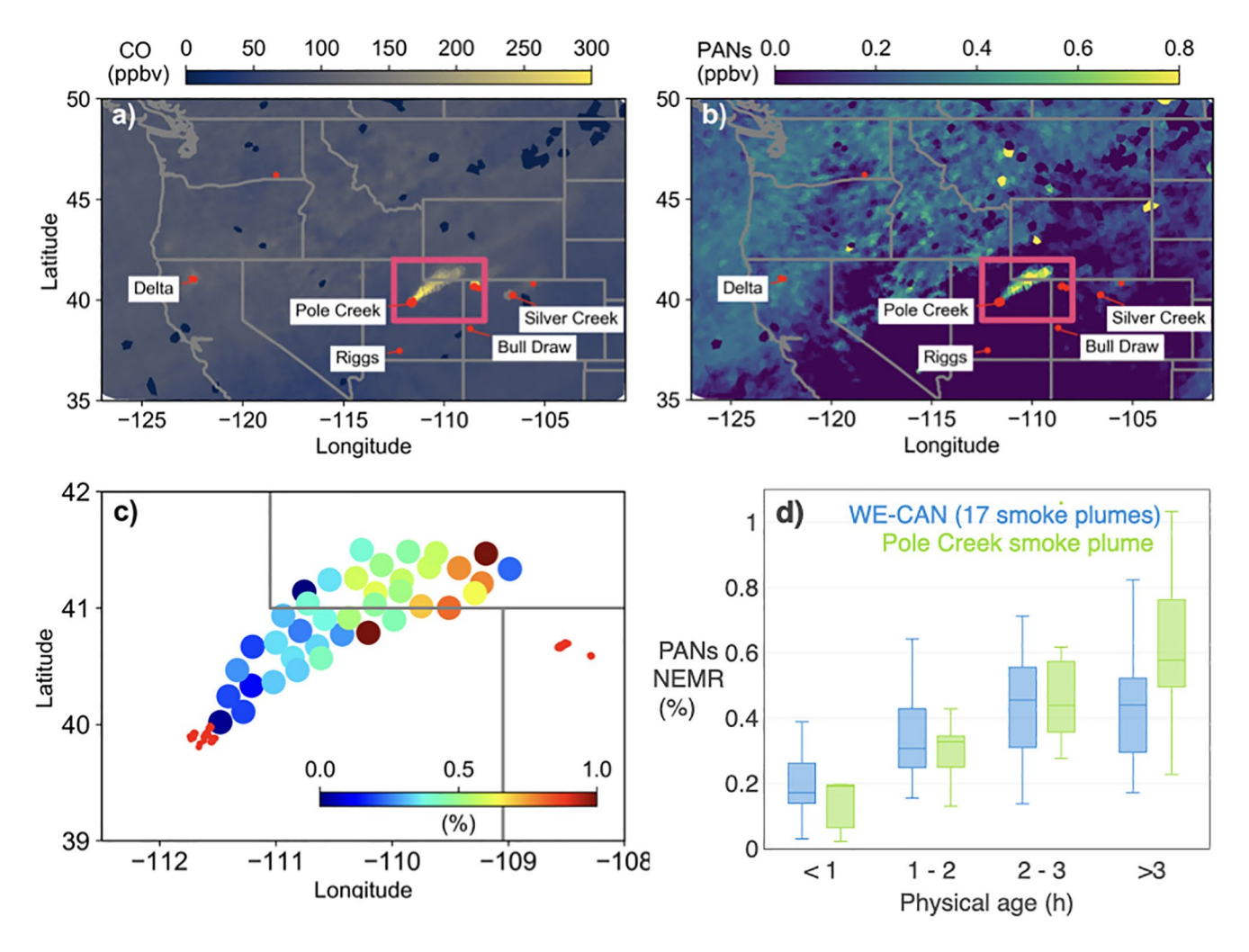


Figure 3. Cross-Track Infrared Sounder (CrIS) (a) CO and (b) peroxynitrates (PANs) retrievals for September 13, 2018. The pink boxes in panels (a) and (b) encompass the region plotted in panel (c). (c) CrIS PANs NEMRs with respect to CO for the Pole Creek Fire Plume. NEMRs are calculated assuming a background of 0.13 and 90 ppbv for PANs and CO, respectively. (d) PANs NEMRs for the Pole Creek Fire (green) calculated with the CrIS data compared to those calculated across 17 fresh plumes associated with known fires sampled in a pseudo-Lagrangian fashion during the WE-CAN campaign (blue), see Juncosa Calahorrano et al. (2020) for details.

3.3. CrIS—Detected PANs Enhancements in Wildfire Smoke Plumes

Figure 3 shows CrIS CO (Figure 3a) and PANs (Figure 3b) retrievals associated with the Pole Creek Fire in Utah. This plume demonstrates that the combined spatial resolution and sensitivity of CrIS is sufficient to detect chemical evolution in plumes when background conditions are favorable for these calculations (i.e., when a plume is isolated and the abundance of PANs and CO within the plume are substantially higher than outside the plume).

On September 13, 2018 high winds drove active burning despite efforts to contain the Pole Creek Fire. The smoke closest to the fire becomes visible in satellite imagery (GOES16 2 km Ch2 HighRes Vis) between 10 a.m. and 10:30 a.m. LT (16:00 and 16:30 UTC); the plume crosses the Utah-Wyoming border at 2 p.m. LT (20:00 UTC). The Suomi NPP overpass shown in Figure 3 is at 2:40 p.m. LT (20:40 UTC) (3.6–4.6 hr after the plume becomes visible).

Figure 3c shows that the PANs NEMR (in percent units) with respect to CO increases in the smoke plume with distance from the fire source, reflecting the photochemical production of PANs. To our knowledge, this is the first time the production of PANs on the timescale of minutes to hours has been observable via satellite. Figure 3d compares the CrIS PANs NEMRs from the Pole Creek Fire smoke plume with those produced from the WE-CAN in situ data set. It shows that the rate of PANs production in the Pole Creek Fire plume is within the range of that



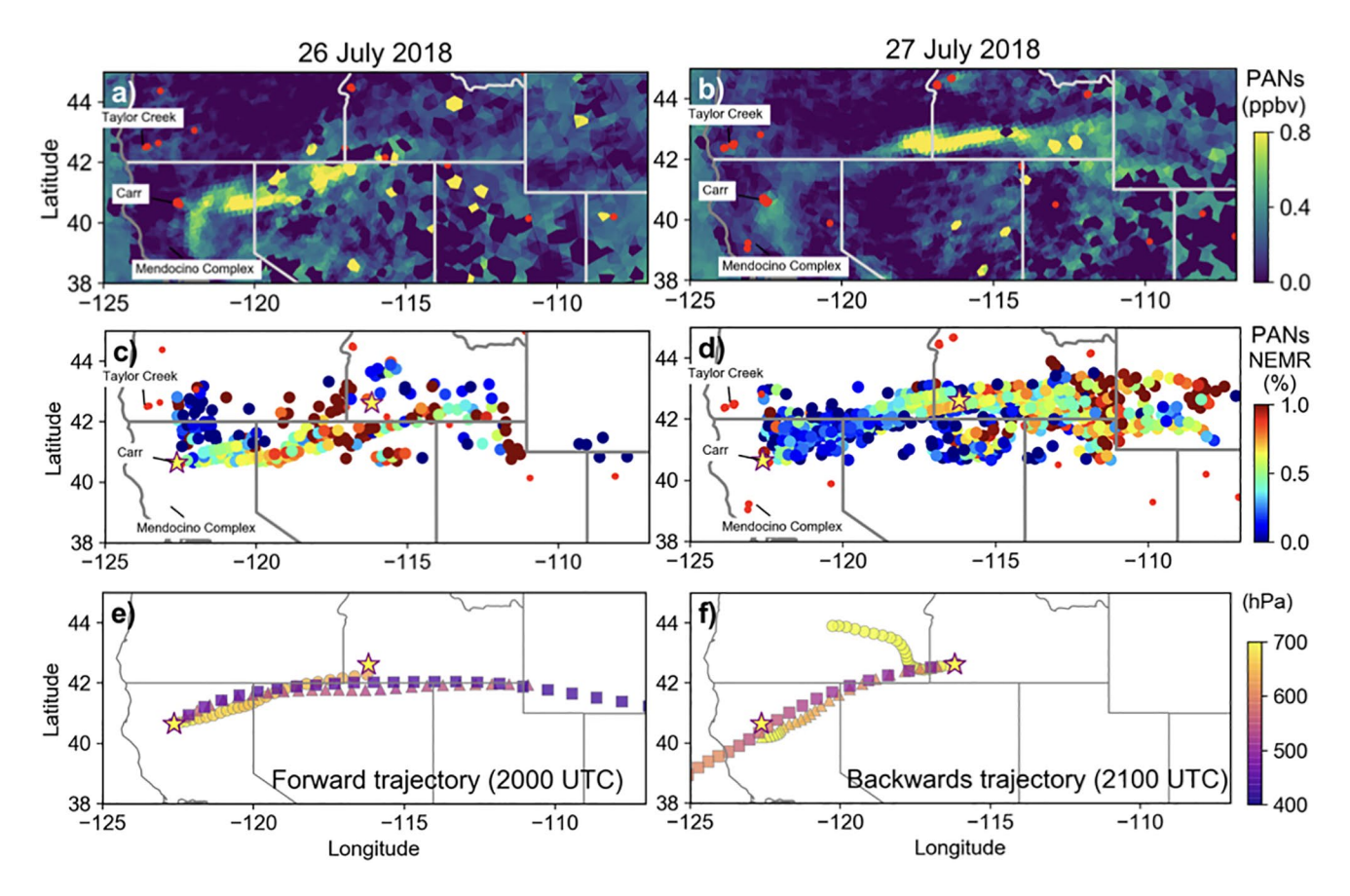


Figure 4. Cross-Track Infrared Sounder (CrIS) peroxynitrates (PANs) retrievals of the Carr Fire smoke plume on (a) July 26, 2018 and (b) July 27, 2018. Panels (c) and (d) show corresponding PANs NEMRs with respect to CO for the Carr Fire plume. Panel (e) presents forward trajectories initialized on July 26, 2018 at the Suomi National Polar-orbiting Partnership (Suomi NPP) overpass time (~20:00 UTC) at the Carr Fire centroid location (40.65°N, 122.63°W) (yellow star to the west). Panel (f) presents backward trajectories initialized on July 27, 2018 at the Suomi NPP overpass time (~21:00 UTC) at (42.63°N, 116.18°W) (yellow star to the east). Trajectories were initialized at 720 (circles), 600 (triangles), and 495 (squares) hPa.

observed for plumes that were sampled during WE-CAN. The CrIS PANs NEMRs increase from 0.2% to 0.4% in \sim 3–4 hr of transport downwind from the fire (see Figure S8 in Supporting Information S1 for uncertainties). Similarly, the WE-CAN PANs NEMRs increase from 0.17% to 0.43% in 3–4 hr of physical aging.

Figure 4 demonstrates the ability of CrIS to detect a wildfire plume over the course of several days. The smoke plume from the Carr Fire is first visible in the CrIS CO and PANs retrievals on July 26, 2018 (Figure 4a). The plume continues to be easily distinguished on July 27, 2018 (Figure 4b) as the fire continued to burn and the smoke from the previous day moved toward the east-northeast. Figures 4a and 4b show the location of the Carr Fire smoke plume over several other downwind states.

Like all wildfires, the injection height of the Carr fire smoke plume was variable, and the CrIS data itself offers limited information on the vertical location of the plume. The NSF/NCAR C-130 sampled the Carr Fire plume on July 26, 2018 at ~23:00 UTC, and the pseudo-Lagrangian sampling of this plume occurred between 665 and 510 hPa. The forward trajectories in panel (e) show that smoke emitted by the Carr Fire on July 26, 2018 would reach southwest Idaho (easternmost yellow star) in 11–24 hr depending on the injection altitude.

A set of backward trajectories initialized at various altitudes from the easternmost star in Figure 4f provide additional constraints on the likely altitude of the smoke detected by CrIS.

We calculated back trajectories initialized at 720 (circles), 600 (triangles), and 495 (squares) hPa at 21:00 UTC, the approximate daytime CrIS overpass time on July 27, 2018. Back trajectories initialized between 600 and 495 hPa are consistent with the transport of the smoke plume visible by satellite. Back trajectories initialized lower (i.e., ~700 hPa) are inconsistent with the visible plume transport pathway.



The trajectories imply that the PANs NEMRs detected on July 27, 2018 by CrIS (at 21:00 UTC) over southwest Idaho are associated with smoke emitted from the Carr Fire at ~3 a.m. LT (~10:00 UTC), when it burned at a lower intensity. The atmospheric temperatures encountered by the smoke favored PANs stability. We use the range of temperatures (288-264 K) from the NARR data at the time and locations of the forward trajectories in Figures 4e and 4a, NO:NO, between 0.15 and 0.30 based on the in situ observations, and an approximate OH concentration of 2×10^6 molecules cm⁻³ to calculate PAN lifetime following Singh (1987). We do not include PAN photolysis in this calculation because this is only important in the upper troposphere, and even in the upper troposphere the lifetime against loss via photolysis is on the order of a month (Fischer et al., 2014; Talukdar et al., 1995). The lifetime against oxidation by OH is also much longer than the lifetime against thermal decomposition, especially during summer. We also note that much of the transport occurred overnight, when these losses do not occur. PAN lifetime (largely against thermal decomposition) ranges between 7.5 and 414 hr depending on injection altitude and the NO:NO, ratio. Higher injection altitudes and lower NO:NO, ratios promote PAN stability. For instance, if we assume that the plume is injected at 720 hPa, the PAN lifetime is \sim 7.5–12 hr. If the plume is injected higher (i.e., 600 (490) hPa) the PAN lifetime is ~60–95 (~300–400) hours. Figure 4 shows that PANs NEMRs in southwest Idaho on July 27, 2018 are comparable to those closer to the Carr Fire centroid on July 26, 2018 (Figure 4c), suggesting PANs conservation and transport over long distances.

4. Conclusions

We present the first analysis of CrIS PANs measurements over North America. We focus our analysis on summer 2018, aligning with in situ observations of wildfire smoke collected by the WE-CAN field intensive. This first analysis of the new CrIS PANs data demonstrates the following.

- CrIS is able to detect PANs and CO enhancements in smoke plumes from individual wildfires following periods of active fire growth. Enhancements in PANs are also present within large multistate scale smoke plumes from regional sets of wildfires
- 2. We segregate and examine the abundance of tropospheric average PANs in smoke-impacted CrIS retrievals using two different satellite-based attribution methods. We find that smoke-impacted retrievals contain significantly higher tropospheric average PANs than smoke-free retrievals based on *t* tests
- 3. An analysis of smoke-impacted CrIS PANs retrievals over the entire study region suggests that wildfires are responsible for approximately 19–56% of the tropospheric PANs over the western U.S. during summer months
- 4. When combined with favorable background conditions, the spatial resolution of CrIS is sufficient to observe the chemical evolution of PANs in wildfire plumes. To our knowledge, this is the first time that rapid photochemical production of PANs is observed from a satellite
- 5. CrIS is able to detect PANs and CO enhancements in plumes that have been transported several hours to days downwind from major wildfires. For example, we can use CrIS to track smoke from the Carr Fire as it moves across several western U.S. states. The Carr Fire produced a large plume when it grew by tens of thousands of acres over several days, and the plume remained intact due to favorable meteorological conditions

This work reinforces the importance of wildfires as a source of PANs to the free troposphere over North America during summer months. It also demonstrates that CrIS measurements of PANs can be used to extend the analysis of recent observational campaigns.

Data Availability Statement

Data used in this study can be found in the Mountain Scholar CSU digital repository (http://dx.doi. org/10.25675/10217/228793). In situ PAN and CO data are available in the WE-CAN data archive (https://data.eol.ucar.edu/master_lists/generated/we-can/).

Acknowledgments

This work was supported by NASA Award Number NNH17ZDA001N-TASN-PP. Part of this work was carried out at the Jet Propulsion Laboratory, California Institute of Technology, under contract to NASA.

References

Akagi, S. K., Yokelson, R. J., Wiedinmyer, C., Alvarado, M. J., Reid, J. S., Karl, T., et al. (2011). Emission factors for open and domestic biomass burning for use in atmospheric models. Atmospheric Chemistry and Physics, 11(9), 4039–4072. https://doi.org/10.5194/acp-11-4039-2011
 Alvarado, M. J., Logan, J. A., Mao, J., Apel, E., Riemer, D., Blake, D., et al. (2010). Nitrogen oxides and PAN in plumes from boreal fires during ARCTAS-B and their impact on ozone: An integrated analysis of aircraft and satellite observations. Atmospheric Chemistry and Physics, 10(20), 9739–9760. https://doi.org/10.5194/acp-10-9739-2010



- Alvarado, M. J., Lonsdale, C. R., Yokelson, R. J., Akagi, S. K., Coe, H., Craven, J. S., et al. (2015). Investigating the links between ozone and organic aerosol chemistry in a biomass burning plume from a prescribed fire in California chaparral. *Atmospheric Chemistry and Physics*, 15(12), 6667–6688. https://doi.org/10.5194/acp-15-6667-2015
- Baylon, P., Jaffe, D. A., Wigder, N. L., Gao, H., & Hee, J. (2015). Ozone enhancement in western US wildfire plumes at the Mt. Bachelor Observatory: The role of NOx. Atmospheric Environment, 109, 297–304. https://doi.org/10.1016/j.atmosenv.2014.09.013
- Beer, R., Bowman, K. W., Brown, P. D., Clough, S. A., Goldman, A., Jacob, D. J., et al. (1999). Tropospheric emission spectrometer (TES) (Vol. 112).
- Bond, T. C., Streets, D. G., Yarber, K. F., Nelson, S. M., Woo, J.-H., & Klimont, Z. (2004). A technology-based global inventory of black and organic carbon emissions from combustion. *Journal of Geophysical Research*, 109(D14), D14203. https://doi.org/10.1029/2003JD003697
- Bowman, K. W., Rodgers, C. D., Kulawik, S. S., Worden, J., Sarkissian, E., Osterman, G., et al. (2006). Tropospheric emission spectrometer: Retrieval method and error analysis. *IEEE Transactions on Geoscience and Remote Sensing*, 44(5), 1297–1307. https://doi.org/10.1109/TGRS.2006.871234
- Brey, S. J., & Fischer, E. V. (2016). Smoke in the city: How often and where does smoke impact summertime ozone in the United States? *Environmental Science & Technology*, 50(3), 1288–1294. https://doi.org/10.1021/acs.est.5b05218
- Briggs, N. L., Jaffe, D. A., Gao, H., Hee, J. R., Baylon, P. M., Zhang, Q., et al. (2017). Particulate matter, ozone, and nitrogen species in aged wildfire plumes observed at the Mount Bachelor Observatory. Aerosol and Air Quality Research, 16(12), 3075–3087. https://doi.org/10.4209/aaqr.2016.03.0120
- Crutzen, P. J., & Andreae, M. O. (1990). Biomass burning in the tropics: Impact on atmospheric chemistry and biogeochemical cycles. *Science*, 250(4988), 1669–1678. https://doi.org/10.1126/science.250.4988.1669
- Draxler, R. R., & Hess, G. D. (1998). An overview of the HYSPLIT_4 modelling system for trajectories, dispersion, and deposition (Vol. 25). Bureau of Meteorology Research Centre.
- Fearnside, P. M., Leal, N., & Fernandes, F. M. (1993). Rainforest burning and the global carbon budget: Biomass, combustion efficiency, and charcoal formation in the Brazilian Amazon. *Journal of Geophysical Research*, 98(D9), 16733. https://doi.org/10.1029/93JD01140
- Fischer, E. V., Jacob, D. J., Yantosca, R. M., Sulprizio, M. P., Millet, D. B., Mao, J., et al. (2014). Atmospheric peroxyacetyl nitrate (PAN): A global budget and source attribution. *Atmospheric Chemistry and Physics*, 14(5), 2679–2698. https://doi.org/10.5194/acp-14-2679-2014
- Fischer, E. V., Zhu, L., Payne, V. H., Worden, J. R., Jiang, Z., Kulawik, S. S., et al. (2018). Using TES retrievals to investigate PAN in North American biomass burning plumes. *Atmospheric Chemistry and Physics*, 18(8), 5639–5653. https://doi.org/10.5194/acp-18-5639-2018
- Fu, D., Bowman, K. W., Worden, H. M., Natraj, V., Worden, J. R., Yu, S., et al. (2016). High-resolution tropospheric carbon monoxide profiles retrieved from CrIS and TROPOMI. Atmospheric Measurement Techniques, 9(6), 2567–2579. https://doi.org/10.5194/amt-9-2567-2016
- Juncosa Calahorrano, J. F., Lindaas, J., O'Dell, K., Palm, B. B., Peng, Q., Flocke, F., et al. (2020). Daytime Oxidized Reactive Nitrogen Partitioning in Western U.S. Wildfire Smoke Plumes. *Journal of Geophysical Research: Atmospheres*, 126, e2020JD033484. https://doi. org/10.1029/2020JD033484
- Lindaas, J., Farmer, D. K., Pollack, I. B., Abeleira, A., Flocke, F., Roscioli, R., et al. (2017). The impact of aged wildfire smoke on atmospheric composition and ozone in the Colorado Front Range in summer 2015. Atmospheric Chemistry and Physics Discussion. [Preprint] https://doi.org/10.5194/acp-2017-171
- Lindaas, J., Pollack, I. B., Garofalo, L. A., Pothier, M. A., Farmer, D. K., Kreidenweis, S. M., et al. (2020). Emissions of reactive nitrogen from Western U.S. wildfires during Summer 2018. *Journal of Geophysical Research: Atmospheres*, 126, e2020JD032657. https://doi.org/10.1029/2020JD032657
- Liu, X., Zhang, Y., Huey, L. G., Yokelson, R. J., Wang, Y., Jimenez, J. L., et al. (2016). Agricultural fires in the southeastern U.S. during SEAC ⁴ RS: Emissions of trace gases and particles and evolution of ozone, reactive nitrogen, and organic aerosol: Agricultural Fires in the SE US. *Journal of Geophysical Research: Atmospheres*, 121, 7383–7414. https://doi.org/10.1002/2016JD025040
- Mu, M., Randerson, J. T., van der Werf, G. R., Giglio, L., Kasibhatla, P., Morton, D., et al. (2011). Daily and 3-hourly variability in global fire emissions and consequences for atmospheric model predictions of carbon monoxide: Daily and hourly global fire emissions. *Journal of Geophysical Research*, 116, D24303. https://doi.org/10.1029/2011JD016245
- Payne, V. H., Alvarado, M. J., Cady-Pereira, K. E., Worden, J. R., Kulawik, S. S., & Fischer, E. V. (2014). Satellite observations of peroxyacetyl nitrate from the Aura Tropospheric Emission Spectrometer. Atmospheric Measurement Techniques, 7(11), 3737–3749. https://doi.org/10.5194/amt-7-3737-2014
- Payne, V. H., Kulawik, S. S., Fischer, E. V., Brewer, J. F., Huey, L. G., Miyazaki, K., et al. (2021). Satellite measurements of peroxyacetyl nitrate from the Cross-Track Infrared Sounder: Comparison with ATom aircraft measurements. *Atmospheric Measurement Techniques Discussions*. [Preprint] https://doi.org/10.5194/amt-2021-353
- Revercomb, H., & Strow, L. (2019). Suomi NPP CrIS level 1B full spectral resolution V2. Accessed from GES DISC. https://doi.org/10.5067/9NPOTPIPLMAW
- Rolph, G. D., Draxler, R. R., Stein, A. F., Taylor, A., Ruminski, M. G., Kondragunta, S., et al. (2009). Description and verification of the NOAA smoke forecasting system: The 2007 fire season. Weather and Forecasting, 24(2), 361–378. https://doi.org/10.1175/2008WAF2222165.1
- Ruminski, M., Kondragunta, S., Draxler, R., Zeng, J., & Rm, A. (2006). Recent changes to the hazard mapping system. In: *Proceedings of the 15th International Emission Inventory Conference* (Vol. 15, p. 18).
- Singh, H. B. (1987). Reactive nitrogen in the troposphere. *Environmental Science & Technology*, 21(4), 320–327. https://doi.org/10.1021/es00158a001
- Singh, H. B., Cai, C., Kaduwela, A., Weinheimer, A., & Wisthaler, A. (2012). Interactions of fire emissions and urban pollution over California: Ozone formation and air quality simulations. *Atmospheric Environment*, 56, 45–51. https://doi.org/10.1016/j.atmosenv.2012.03.046
- Singh, H. B., & Hanst, P. L. (1981). Peroxyacetyl nitrate (PAN) in the unpolluted atmosphere: An important reservoir for nitrogen oxides. Geo-physical Research Letters, 8(8), 941–944. https://doi.org/10.1029/GL008i008p00941
- Talukdar, R. K., Burkholder, J. B., Schmoltner, A.-M., Roberts, J. M., Wilson, R. R., & Ravishankara, A. R. (1995). Investigation of the loss processes for peroxyacetyl nitrate in the atmosphere: UV photolysis and reaction with OH. *Journal of Geophysical Research*, 100(D7), 14163–14173. https://doi.org/10.1029/95JD00545
- Yokelson, R. J., Crounse, J. D., DeCarlo, P. F., Karl, T., Urbanski, S., Atlas, E., et al. (2009). Emissions from biomass burning in the Yucatan. Atmospheric Chemistry and Physics, 9, 5785–5812. https://doi.org/10.5194/acp-9-5785-2009